AGU PUBLICATIONS

Geochemistry, Geophysics, Geosystems

TECHNICAL BRIEF

10.1002/2014GC005289

Key Points:
- Ar-Ar geochronology
- Sample transfer furnace system
- Ar-Ar dating of whole-rocks and young samples

Supporting Information:
- ReadMe
- tso1

Correspondence to:
J. A. Pfänder,
pfaender@tu-freiberg.de

Citation:
Pfänder, J. A., B. Sperner, L. Ratschbacher, A. Fischer, M. Meyer, M. Leistner, and H. Schaeben (2014), High-resolution $^{40}Ar/^{39}Ar$ dating using a mechanical sample transfer system combined with a high-temperature cell for step heating experiments and a multicollector ARGUS noble gas mass spectrometer, *Geochem. Geophys. Geosyst.*, *15*, doi:10.1002/2014GC005289.

Received 11 FEB 2014
Accepted 6 MAY 2014
Accepted article online 10 MAY 2014

High-resolution $^{40}Ar/^{39}Ar$ dating using a mechanical sample transfer system combined with a high-temperature cell for step heating experiments and a multicollector ARGUS noble gas mass spectrometer

Jörg A. Pfänder[1], Blanka Sperner[1], Lothar Ratschbacher[1], Albrecht Fischer[2], Martin Meyer[3,4], Martin Leistner[3], and Helmut Schaeben[3]

[1]TU Bergakademie Freiberg, Geologie, Freiberg, Germany, [2]CreaTec Fischer & Co. GmbH, Erligheim, Germany, [3]TU Bergakademie Freiberg, Geophysik und Geoinformatik, Freiberg, Germany, [4]Now at TU Dresden, Abfallwirtschaft und Altlasten, Pirna, Germany

Abstract $^{40}Ar/^{39}Ar$ dating of young (<1 Ma) and/or low potassium samples requires degassing of large amounts of material either by a laser or a furnace. A furnace excels in precise and reproducible temperature control and in providing a homogeneous temperature distribution even for relatively large sample amounts. For most systems, however, the degassed mineral or whole-rock residues remain in the crucible after measurement. This reduces the thermal conductivity and increases the blank levels and baking times. To mitigate these problems, we combined a mechanical sample transfer system with a low volume (~90 mL) high-temperature cell. The system operates under ultrahigh vacuum and uses Mo-crucibles, in which up to 1000 mg of sample is transferred into the furnace and taken out after degassing. The system has short baking times (20–30 min), highly reproducible heating conditions and an overall low blank level due to the absence of silicate (glassy) sample residue in the main crucible of the furnace. The system interconnects through a gas purification line with a low volume, high sensitivity multicollector ARGUS noble gas mass spectrometer. Intraday reproducibility of $^{40}Ar/^{36}Ar$ ratios measured on air aliquots of $>5 \times 10^{-16}$ mol ^{36}Ar is better than 0.5‰–1.0‰ (1σ, $n = 4$–8). We illustrate the system performance by $^{40}Ar/^{39}Ar$ dating of whole-rock samples and mineral separates from the Oman ophiolite as well as from the Siebengebirge, Heldburg, and Rhön volcanic provinces in Central Germany.

1. Introduction

$^{40}Ar/^{39}Ar$ dating is widely applied to obtain radioisotopic ages and thermal histories of geologic processes from extraterrestrial and terrestrial K-bearing rocks and minerals [see *McDougall and Harrison*, 1999, for a review]. The isotope composition of the thermally released Ar from a neutron-irradiated sample supplies the required age information. The potassium content of a sample is hereby determined indirectly by the measured ^{39}Ar, which has been produced by the $^{39}K(n,p)^{39}Ar$ reaction during neutron irradiation. Step wise Ar release by incremental heating provides a number of individual ages from a single sample and allows an internal control on the robustness of the derived age.

Commonly, a thermal laser or a vacuum furnace suitable to reach temperatures >1700°C achieves the step heating in ultrahigh vacuum. A critical issue during heating is the temperature control of the individual heating steps. In most laser heating experiments, the laser power provides a relative measure for the temperature during degassing. This approach makes laser heating unreliable for the determination of Ar diffusion parameters and closure temperatures of minerals [*Dodson*, 1973], or the application of the multidomain diffusion (MDD) analysis of feldspars [e.g., *Lovera et al.*, 1989, 1991]. This problem is mitigated by the use of thermocouples and pyrometer systems [*Cassata and Renne*, 2013], but their application and calibration is complex. The limited mass of sample that can be degassed and the temperature gradient within an unwrapped sample produced by the unidirectional heat supply further hampers thermal laser dating of very young and/or K-poor samples. Although wrapping the sample into Mo foil or Pt-Ir alloy foil and/or movement of the laser beam over a sample in part limit these shortcomings, a homogeneously distributed and constant temperature over a defined period of time (i.e., thermal equilibrium) is difficult to achieve. Tests made in our lab on unwrapped, 80–250 μm

© 2014. American Geophysical Union. All Rights Reserved.

micas loaded on a copper sample holder showed that in >1 mm thick layers the minerals facing the laser beam melt while the underlying minerals remain visibly unaffected.

Using a furnace with thermocouples and temperature control circumvents most of these problems albeit on the expense of a higher system volume and higher blank levels. Additionally, most furnace systems used in $^{40}Ar/^{39}Ar$ dating have the disadvantage that wrapped or unwrapped samples remain and accumulate in the crucible after degassing. This leads to a successive decrease in heat transfer from the crucible to the sample and thus to erroneous temperature measurements over time. In addition, successively longer baking times of the furnace are required to keep the blank level low. Evaporated sample-wrapping material (Al-foil or Cu-foil) also leads to a contamination of the colder parts of the furnace with porous metallic precipitates having an extremely large surface, and thus enlarging the blank level. Other disadvantages arise from chemical disequilibrium between the silicate (glassy) residue in the crucible and the newly added sample material. This disequilibrium may cause chemical reactions during heating (i.e., ion exchange). It thus affects the degassing behavior of the measured phases, potentially influencing the results, with serious consequences in particular in diffusion experiments.

To minimize the volume and to reduce baking times and blank levels of our furnace system, we developed a mechanical system that allows to transfer a sample loaded in a Mo-crucible under ultrahigh vacuum conditions into a low-volume high-temperature cell (HTC) for incremental heating, and to remove the crucible with the residue after degassing. The major advantages of the system are the highly reproducible temperature controlled degassing of the sample, the absence of glassy residue in the main crucible of the HTC and hence very short baking times (20–30 min) and consistently low blank levels.

2. Technical Description

The $^{40}Ar/^{39}Ar$ geochronology facility in Freiberg (Argonlab Freiberg, ALF) is equipped with two independently used ARGUS noble gas mass spectrometers, each connected to a low-volume sample preparation system. Unit I uses a CO_2 laser and a furnace system for sample heating, and a GV Instruments ARGUS noble gas mass spectrometer equipped with five fixed faraday cups for static Ar isotope analysis. The New Wave CO_2 laser is a floating 30 W system with a wavelength of 10.6 μm and a beam diameter adjustable between 0.18 and 3.00 mm. The furnace system and the laser connect to the same preparation system. Unit II is a laser ablation system using a 193 nm ArF excimer laser for spot dating. The sample chamber is connected to a Thermo ARGUS VI noble gas mass spectrometer through a preparation system.

2.1 Furnace System

2.1.1. Sample Chamber and Mechanical Sample Transfer System

The sample chamber (Figures 1a and 1b) is pumped by a Pfeiffer TMU262 turbo pump backed by an oil free diaphragm pump and contains a turntable with 29 counterborings. These take up the Mo-crucibles containing the samples. Positioning of the turntable is achieved manually via a hand wheel and a vacuum feed through. The size of a sample crucible is 6 mm inner and 8 mm outer diameter, at an outer length of 30 mm (volume ~0.8 mL; Figures 1a and 1b). This allows a take-up of ≤1000 mg, dependent on sample type and grain size. The weight of an empty crucible is ~7 g.

The mechanical sample transfer system is assembled on top of the sample chamber on a CF63 flange (Figures 1a and 1b). A steel rod inside the transfer system tube holds a grabber which can be opened and closed by turning a ring magnet on the outer side of the transfer system tube (Figures 1a and 1b). The grabber enables to pick up a sample crucible. A groove in the crucible fixes it in its position. Over a bore in the sample storage turntable (Figure 1e), the crucible is lowered into the HTC by manually moving the magnet on the outer side of the transfer system tube down. Bearings on the bottom of the sample chamber and on top of the HTC (within the connector, Figure 1a) hold the transfer rod and the crucible in a centered position. The crucible passes through a gate valve mounted between the sample chamber and the connector of the HTC, and is placed in a Mo-cavity at the bottom of the main Ta-crucible (Figure 1a). After positioning, the grabber is opened and moved back into its starting position. A screw mounted on the lower end of the transfer system tube allows adjusting the transfer rod into a centered position relative to the bearing in the sample chamber.

© 2014. American Geophysical Union. All Rights Reserved.

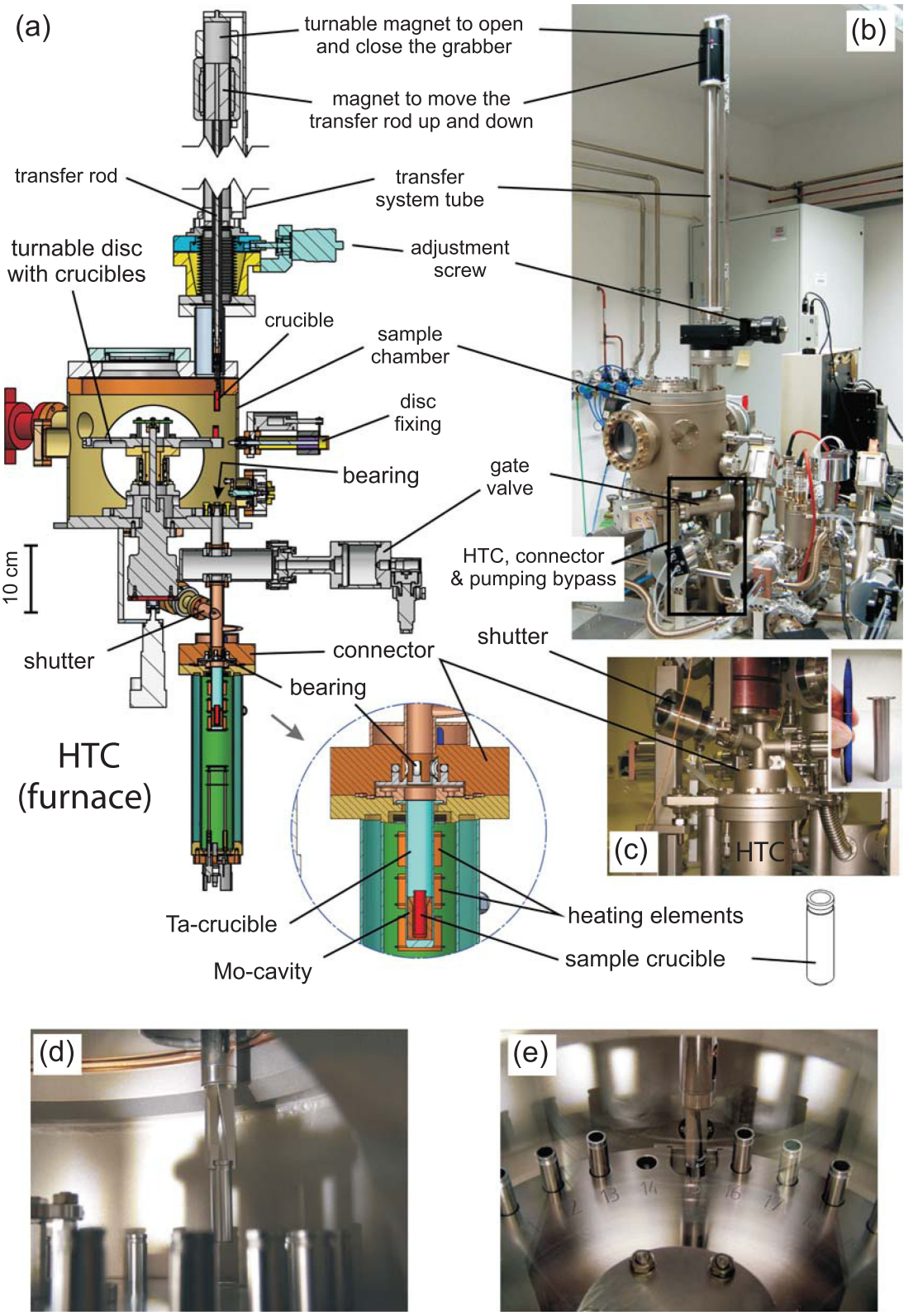

Figure 1. (a, b) Mechanical sample transfer system, sample chamber, and high-temperature cell (HTC; from top to bottom). (c) Upper part of the HTC with connector and shutter. The HTC and connector are water-cooled. Inset: Ta-crucible that separates outer and inner volume (vacuum) of the HTC. (d) Grabber with sample crucible. (e) Turntable with sample crucibles and grabber with crucible passing the turntable downward to the HTC.

© 2014. American Geophysical Union. All Rights Reserved.

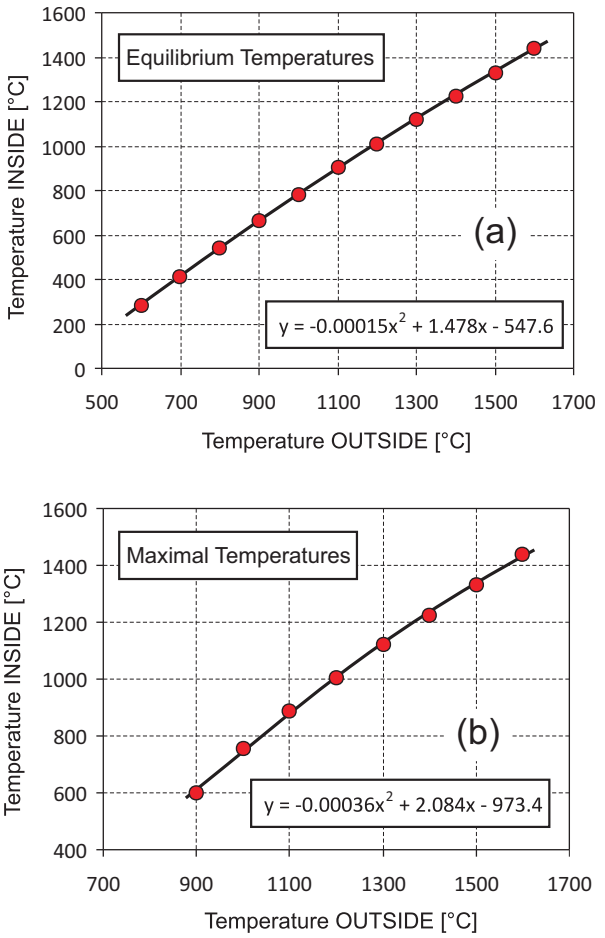

Figure 2. Temperature inside a sample crucible at a given outside temperature, measured between the main Ta-crucible and the heating elements (see Figure 1). (a) Equilibrium temperature. (b) Maximal temperature reached after 3 min ramp time (100°C/min) and 10 min hold time (details see text).

2.1.2. High-Temperature Cell (HTC)

The HTC used for step heating experiments is a differentially pumped, water-cooled, low volume (~90 mL, including connector; see Figure 1a) resistance furnace that allows temperatures up to 1700°C. This temperature is limited by the tungsten-bornitride heating elements that can optionally be replaced by a tungsten heating-foil to allow temperatures up to 2000°C. The heating element encloses a Ta-crucible (inner diameter = 16 mm, inner length = 89 mm, volume 17.9 mL; Figure 1c inset) that isolates the inner from the outer volume. Inside the Ta-crucible sits a Mo-cavity that takes up the sample crucible (Figure 1a, enlargement). A Pfeiffer TMU071 turbo pump backed by an oil free diaphragm pump evacuates the outer volume of the HTC. The inner volume is connected to the sample chamber and the preparation system through a water-cooled connector (Figure 1c). A movable, thin metal shim (shutter), part of the connector, is positioned between the gate valve of the sample chamber and the HTC and is closed after sample transfer has been completed. This shutter protects the valve from heat radiation and vapor condensation during heating (Figures 1a and 1c). The HTC is mounted to the connector by a differentially pumped flange having two copper gaskets. The volume between the gaskets is part of the outer volume of the HTC. A bypass connected to the pumping system of the preparation system achieves the pumping of the inner volume (Figure 1b). Two tungsten-rhenium thermocouples (type C)—positioned between the Ta-crucible and the heating elements—allow a reproducible and stable temperature control. Temperature stability on a defined target temperature is <0.1°C. Target temperatures are ramped using a heating rate of 100°C/min.

Due to a relatively high thermal mass of the crucible system, the heating rate and temperature *inside* a sample crucible deviate from the heating rate and temperature measured by the thermocouples (see Figure 2 and Appendix A). Measured temperatures are thus corrected for according to the temperature calibration diagram shown in Figure 2, achieved by placing a thermocouple inside an empty sample crucible. As shown in Appendix A, more time is required to reach thermal equilibrium between the heating element and the inner part of the crucible for lower target temperatures than for higher temperatures. This needs to be considered in any experiment that requires thermal equilibrium and the knowledge of a precise temperature.

2.1.3. Sample Crucible Blanks

The sample crucibles are made of pure polycrystalline molybdenum (>99.97%). Given the relatively high manufacturing costs, cleaning of used crucibles is reasonable and is performed using hydrofluoric acid as described in Appendix B. After cleaning, the crucibles are baked in UHV for >30 min at >1500°C. Baking is

© 2014. American Geophysical Union. All Rights Reserved.

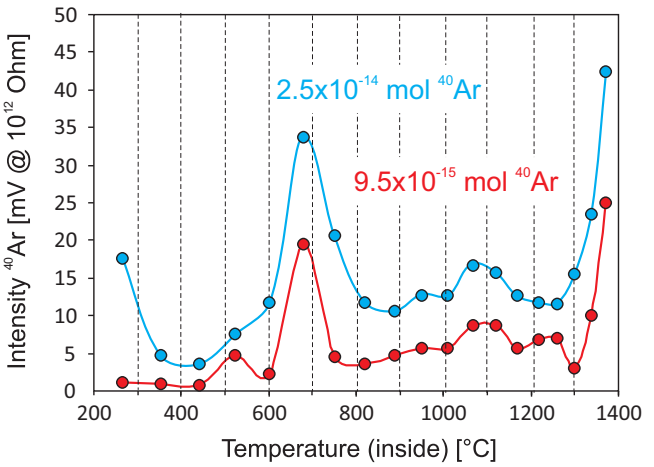

Figure 3. Argon release patterns of two molybdenum crucibles (sample crucibles) measured after baking in UHV at 1500°C for 30 min. Red curve: degassing curve of a crucible stored a few days under UHV after baking. Blue curve: degassing curve of a crucible stored for 26 days in air after baking. Numbers denote total amount of ^{40}Ar released from the crucibles. Ar release is not continuous, most of the Ar releases at ~680°C, likely corresponding to the activation temperature of Ar desorption from the grain boundaries and lattice defects in polycrystalline molybdenum (the increase at >1300°C results from insufficient baking).

also required for new crucibles. After baking, the crucibles will take up Ar from the air, even when stored under UHV. The typical total Ar content of a crucible after baking depends on the storage time and is in the order of 7–9 $\times$ 10^{-15} mol ^{40}Ar (for calculating moles from signal intensities see Appendix C). In Figure 3, Ar release patterns of baked crucibles are shown after different storage times in air and under UHV. The maximum Ar release rate is observed at temperatures of ~680°C and >1300°C. Ar uptake rates are nearly linear over a period of several weeks, and are ~6 $\times$ 10^{-16} mol ^{40}Ar per day under atmosphere (determined over a period of 10 days) and ~1.3 $\times$ 10^{-16} mol ^{40}Ar per day under UHV (determined over a period of 26 days).

2.2. ARGUS Noble Gas Mass Spectrometer

Isotope analyses of Ar are performed on a GV Instruments ARGUS noble gas mass spectrometer. Appendix D, E, and Figure 4 provide details about gas purification, hardware integration, and system automation, respectively. The ARGUS is equipped with a modified Nier-type electron bombardment source, providing a sensitivity between 1.1 and 1.3 $\times$ 10^{-3} A/Torr (<3 $\times$ 10^{-14} mol/V) at a trap current of 208 μA [see also *Mark et al*., 2009]. The collector array consists of five faraday cups in fixed positions for a simultaneous measurement of all five Ar isotopes (Figure 5). A 10^{11} Ohm resistor is used on mass position 40 and 10^{12} Ohm resistors are used on mass positions 36–39. Mass resolution is about 200 at an acceleration voltage of 4.5 kV. Gain stability of the amplifiers determined over a period of 12 months is between 7 and 20 ppm (1σ, $n = 9$). Baseline drifts are 0.0015, 0.0017, 0.0007, −0.0025, and −0.0013 mV/h on the L2 (36), L1 (37), Ax (38), H1 (39), and H2 (40) amplifiers, respectively, at noise levels between 2 and 6 $\times$ 10^{-5} V (1σ; Figure 6). The static rise is between 6.6 $\times$ 10^{6} and 3.4 $\times$ 10^{7} atoms ^{40}Ar/min (1.1–5.6 $\times$ 10^{-17} mol/min) and ~6.6 $\times$ 10^{5} atoms ^{36}Ar/min (1.1 $\times$ 10^{-18} mol/min) at typical system blanks of <2.5 $\times$ 10^{-16} mol ^{40}Ar and <8.1 $\times$ 10^{-18} mol ^{36}Ar. Air aliquot measurements yield ^{40}Ar/^{36}Ar ratios between 298 and 306, dependent on source adjustment. Intraday reproducibility is typically better than 1.0‰ (1σ, $n = 4$–8) at ^{36}Ar intensities >20 mV on 10^{12} Ohm (5.6 $\times$ 10^{-16} mol; Figure 7). For a more detailed description of the performance of the ARGUS, see *Mark et al*. [2009].

2.3. Data Management and Data-Reduction Software

The core of our data management system is a MySQL database running on a web server (Figure 8). An in-house developed Matlab software package manages data handling and reduction. Gain corrected raw data (blank, sample, and airshot measurements), stored in ASCII and Excel® files on a local hard disk by the data acquisition software of the mass spectrometer, are automatically transferred to the MySQL database and linked with the related sample and irradiation information provided in a separate ASCII file (*.irr - file, comprises date and time of irradiation, irradiation position, sample origin, sample owner, mineral type, and weights; Figure 8). The main Matlab program (*gcalcage*), employing a graphical user interface, extracts all the required data of an experiment from the database to perform time-zero regression, intercept calculation, correction for mass discrimination and interfering isotopes, as well as age and *J* value calculation. In a first step, *gcalcage* displays sequentially the regression analysis for all masses of each temperature step with the option to eliminate outliers and to select different fit models (linear, quadratic, exponential, and power).

© 2014. American Geophysical Union. All Rights Reserved.

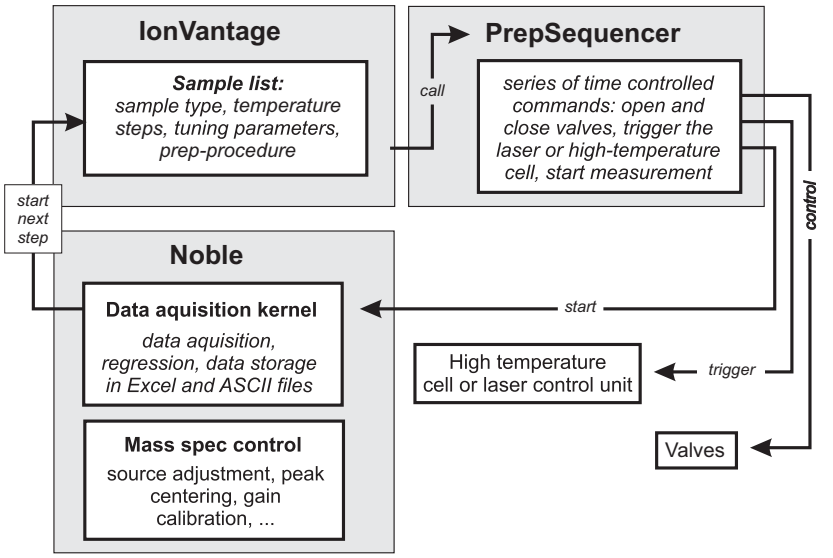

Figure 4. Schematic drawing of the hardware control and data acquisition system. The major software unit is a program packet delivered by GV Instruments (gray), comprising the Noble, IonVantage, and PrepSequencer modules. Triggered by IonVantage, the PrepSequencer executes a series of commands, i.e., to wait for processes to be finished, control valves, trigger the laser or high temperature cell (HTC), and start the data acquisition process. All procedures are time controlled, i.e., no feedback is given by the laser or HTC control unit after having finished a heating step.

In a second step, *gcalcage* presents the results in various plots (%^{40}Ar* and K/Ca-ratio versus cumulative ^{39}Ar, age spectrum, isochron and inverse isochron diagrams) and allows to select or deselect individual temperature steps to be included in the calculation and to adapt the initial ^{40}Ar/^{36}Ar value used to calculate the age spectrum. An export function lists all relevant data, which can be copied into MS Excel® to enable the use of Isoplot [*Ludwig*, 2012]. Parameters that commonly experience slight adaptations due to ongoing research (e.g., decay constants, fluence-monitor reference ages, interference correction factors, etc.) are not stored in the database but extracted by *gcalcage* from a separate parameter file, *gcalcage* calculates errors based on a differential error-propagation algorithm and by using the intercept errors and the errors given with the constants in the parameter file as starting values. Based on the sample type, *gcalcage* provides either ages or *J* values. The latter are automatically transferred to the database and assigned to the corresponding samples, irradiated on the same irradiation plate.

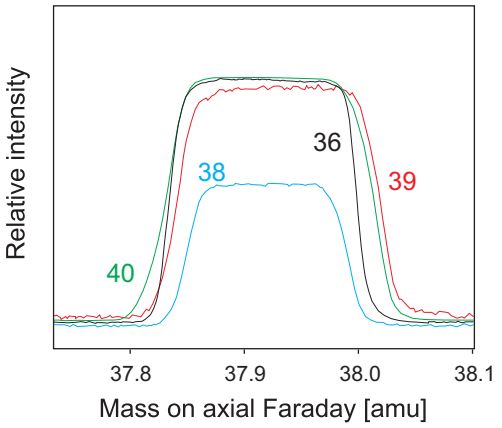

Figure 5. Typical peak shapes and coincidence of masses for the ARGUS noble gas mass spectrometer of the Freiberg Argon facility. Signal intensities are ^{40}Ar(H2) = 3216 mV, ^{39}Ar(H1) = 36 mV, ^{38}Ar(Ax) = 20 mV, and ^{36}Ar(L2) = 99 mV.

From air-aliquot measurements, *calcairshots* calculates the sensitivity and the mass bias of the ion source, adopting linear mass-dependent isotope fractionation. Both values and associated errors are stored in the database and retrieved by *gcalcage* for age and *J* value calculations. Appropriate mass-bias correction factors are selected automatically based on date and time of sample and airshot measurements.

3. Application and Discussion

Precise age determination applying the ^{40}Ar/^{39}Ar method requires apart from an appropriate hardware a careful sample selection and treatment prior to irradiation

© 2014. American Geophysical Union. All Rights Reserved.

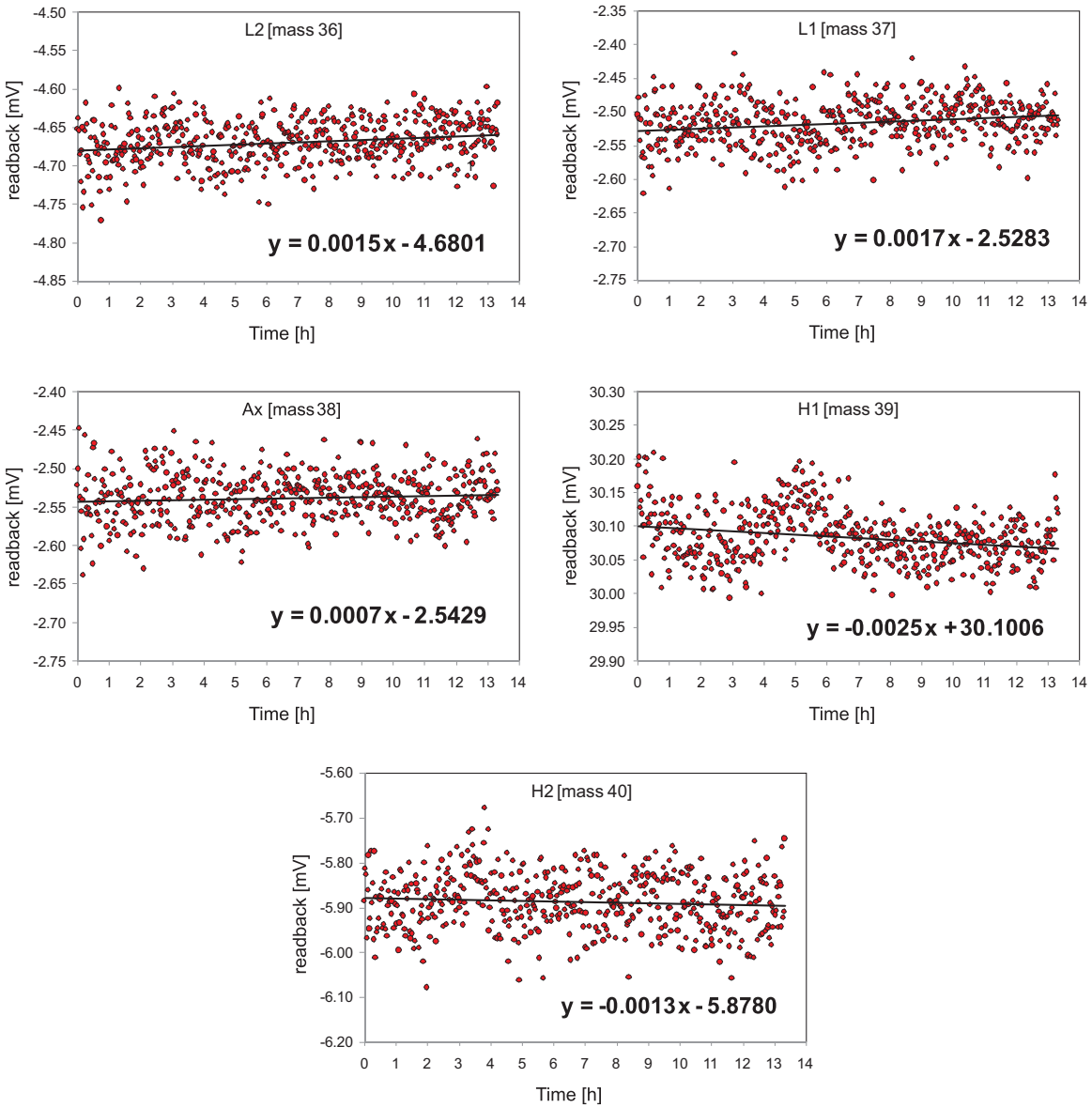

Figure 6. Amplifier noise and baseline drifts over time. Drifts are 0.0015, 0.0017, 0.0007, −0.0025, and −0.0013 mV per hour at noise levels (1σ) between 2 and 6 × 10^{-5} V.

and measurement. Separation of minerals from plutonic and phenocryst-bearing volcanic rocks, followed by hand picking and cleaning in deionized water and/or organic solvents in an ultrasonic bath is the main means in an effort to obtain high-quality data. An example of how careful sample selection and preparation, including leaching in diluted HF, may improve the quality of the obtained ages is given in *Jourdan et al.* [2009]. From two plagioclase fractions (150–210 μm and 210–315 μm) from a single sample, only the finer one provided a well-defined plateau comprising 100% of the released ^{39}Ar, whereas the coarser fraction, affected by alteration, provided a perturbed (bell-shaped) age spectrum indicating significant ^{40}Ar-loss and thus resulting in a slightly lower age.

3.1. Dating of Phenocryst-Free Volcanic Rocks

In cases, where K-bearing phenocrysts are absent in volcanic rocks, ^{40}Ar/^{39}Ar dating requires unaltered whole-rock fragments. In altered whole-rocks, where secondary minerals affected by variable degrees of

© 2014. American Geophysical Union. All Rights Reserved.

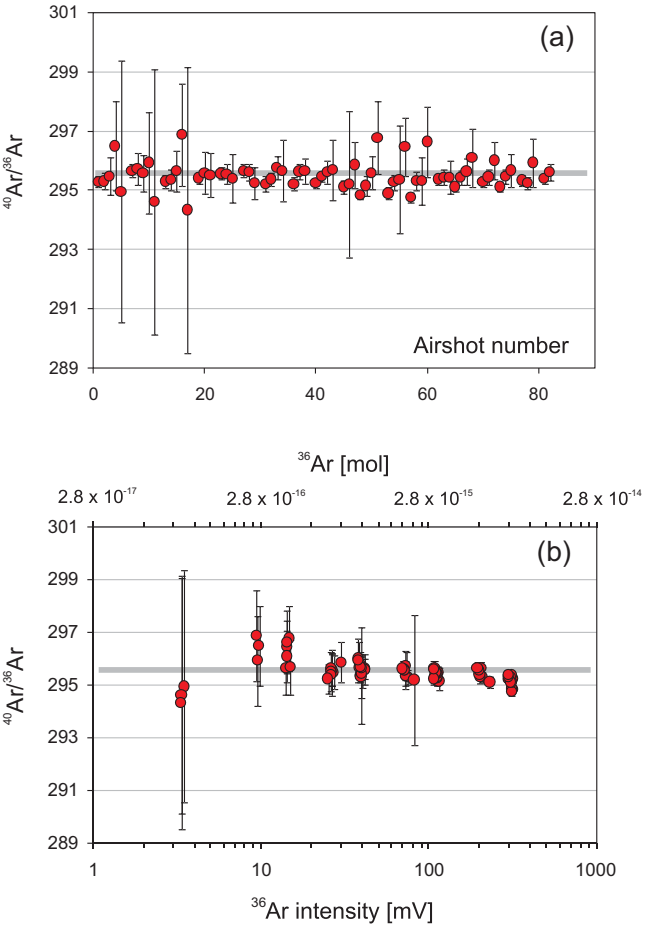

Figure 7. Airshots measured over a period of 6 months. (a) Chronological order, intraday averages renormalized to an atmospheric $^{40}Ar/^{36}Ar$ of 295.5 (thick gray line; $\sigma = 0.15\%$). (b) Renormalized values shown as a function of signal intensity. Error bars are 1σ.

^{40}Ar-loss are present, step heating experiments will lead to a superimposed degassing of primary (undisturbed) and secondary (disturbed) phases, leading to perturbed age spectra and scattered isochron plots. Due to this and the potential loss of ^{39}Ar during irradiation owing to recoil effects, dating of whole-rock samples (or of groundmass fragments) is often regarded as unreliable [e.g., *Duncan et al.*, 1997; *Jourdan et al.*, 2007]. An option to mitigate this problem is to measure a large number of temperature steps (high-resolution incremental heating), in an attempt to separate isotopically different gas fractions from distinct (i.e., altered versus primary) phases. *Koppers et al.* [2004] applied this technique to altered submarine basalts using a thermal CO_2 laser. However, the unknown temperature distribution within a sample during laser heating curtails this approach. In contrast, the highly reproducible conditions in the described furnace system provide the potential for an improved thermal separation of phase specific (and isotopically distinct) gas fractions. This may result in a larger spreading of the data in isochron diagrams as described in *Jourdan et al.* [2012]. These authors compared data from laser and furnace step heating experiments on young Hawaiian basalts, and the larger spread of the furnace data led to a higher precision of both age and initial argon isotope composition.

Figure 9a shows the age spectrum obtained from 51.6 mg of groundmass from a phonolite from the Heldburg region, SE-Germany. The bell-shaped age spectrum indicates ^{40}Ar-loss, hence the age of 14.9 $\pm$ 0.1 Ma derived from only 46.8% of the released ^{39}Ar is a minimum age. 51.8 mg of amphibole, separated from the same sample, yielded a significantly better constrained, although within error identical age of 15.0 $\pm$ 0.1 Ma (93.3% ^{39}Ar; Figure 9b). This demonstrates that "mini-plateaus" (50–70% ^{39}Ar) [*Jourdan et al.*, 2009] from groundmass (whole-rock) samples obtained by high-resolution dating may provide a correct age, but need careful independent control.

© 2014. American Geophysical Union. All Rights Reserved.

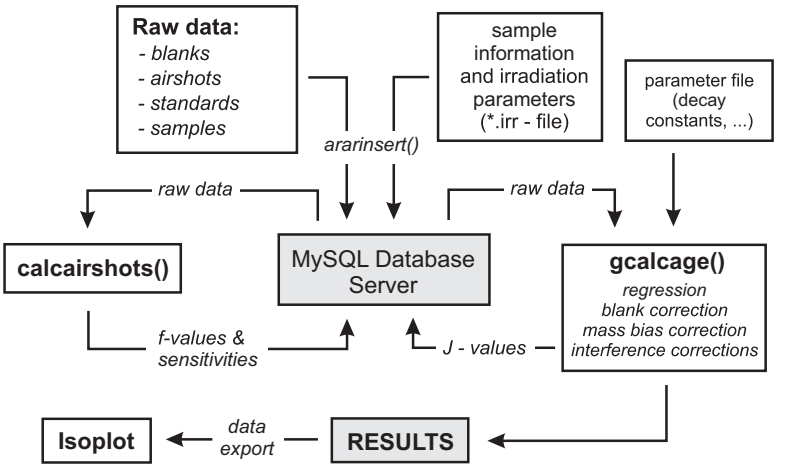

Figure 8. Process chart of data management system. Raw data along with irradiation parameters are stored in a MySQL database system. The Matlab program *calcairshots* calculates the mass discrimination and sensitivities from airshot measurements and stores these data in the database (*f* values and sensitivities). The Matlab program *gcalcage* does time series regression analysis, blank, mass bias, and interference corrections, visualizes the results (age spectrum, isochron, and inverse isochron diagrams) and stores them in tables. The data output can be copied into a Microsoft Excel spreadsheet to be used in Isoplot [*Ludwig*, 2012] for age calculation and data representation.

The age spectrum obtained from 49.7 mg of tephriphonolite from the Siebengebirge volcanic province in Central Germany (Figure 9c) indicates ^{40}Ar-loss for the low-temperature steps, but provides a plateau for the middle-temperature and high-temperature steps with an age of 25.6 $\pm$ 0.1 Ma (1σ) from 77.6% of the ^{39}Ar released. The inverse isochron of the plateau steps yields an identical age and an initial ^{40}Ar/^{36}Ar of 296.4 $\pm$ 6.1 (Figure 9d), corresponding within error to the atmospheric value of 295.5 used for the calculations. This example demonstrates that a large number of temperature steps may provide a solution to separate gas fractions from disturbed and undisturbed phases from aphyric volcanic rocks.

3.2. Dating of Mineral Separates

Step heating of small amounts ($\leq$3 mg in our lab) of K-rich samples can easily be achieved using a defocused laser beam. In contrast, K-poor and/or very young samples ($<$1 Ma) require larger amounts of material. This is also the case if isotope measurements are done on Faraday only machines such as the ARGUS. On the expense of a limited sensitivity, Faraday cups provide an excellent dynamic range and linearity if compared to electron multipliers, and are easy to intercalibrate for static measurements [see *Coble et al.*, 2011, for a discussion on the intercalibration of Faraday cups and electron multipliers in noble gas mass spectrometry].

Figure 9e displays the age spectrum of 19.2 mg amphibole from a basanite from the Rhön volcanic province, Central Germany. The plateau comprises 95.2% of the released ^{39}Ar and provides an age of 24.1 $\pm$ 0.2 Ma. The inverse isochron provides an identical age and an initial ^{40}Ar/^{36}Ar value of 295.5 $\pm$ 1.7 (Figure 9f), indistinguishable from the atmospheric value. Figures 9g and 9h illustrate the age spectrum and inverse isochron diagram of 12.2 mg K-feldspar from a latite from the Siebengebirge in Central Germany. The plateau age of 25.4 $\pm$ 0.1 Ma—comprising 97.7% of the released ^{39}Ar—underlines the performance of the new system for dating "conventional" mineral phases.

Figure 9i displays the age spectrum of 192.1 mg of K-poor amphibole (K = 0.02 wt%) separated from a plagiogranite from the Oman ophiolite. The age spectrum provides a plateau with an age of 94.6 $\pm$ 0.7 Ma comprising 90.6% of the released ^{39}Ar. The inverse isochron age of all steps (94.5 $\pm$ 0.8 Ma, initial ^{40}Ar/^{36}Ar = 296.3 $\pm$ 4.1; Figure 9j) is consistent with the plateau age. Thin section and EMP analysis revealed that the investigated amphiboles consist of magnesio-hornblende that is partly replaced by actinolite forming rims or patches, and likely grown as a secondary phase during hydrothermal alteration or metamorphic overprint. The age spectrum in Figure 9i enables distinguishing two subplateaus. Although close to the analytical resolution, these are statistically significant within the 1σ error level of the calculated ages. These subplateaus might be interpreted as representing the formation/cooling age of the actinolite, degassing at lower temperatures, and the cooling age of the (magmatic) magnesio-hornblende, degassing at higher temperatures.

© 2014. American Geophysical Union. All Rights Reserved.

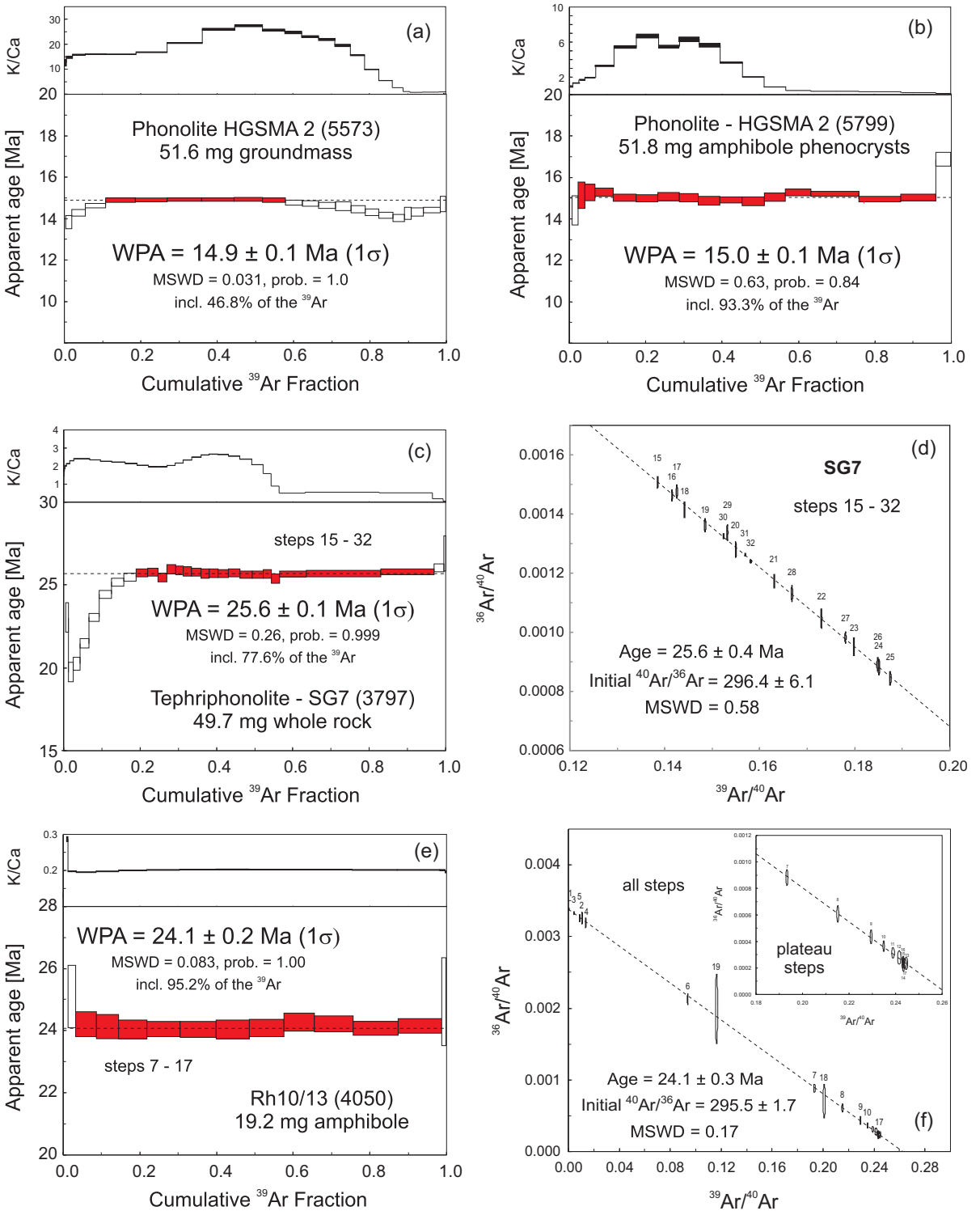

Figure 9. Results of $^{40}Ar/^{39}Ar$ dating using the new furnace system at ALF. (a) Age spectrum of a phonolite groundmass sample from the Heldburg region, Germany, and (b) age spectrum of amphibole phenocrysts isolated from the same sample. The amphiboles provide a significantly more robust plateau comprising 93.3% of the released ^{39}Ar [from M. Abratis et al., Geochemical composition, petrography and $^{40}Ar/^{39}Ar$ age of the Heldburg Phonolite: Implications on magma mixing and mingling, submitted to *International Journal of Earth Sciences*]. (c, d) 49.7 mg whole-rock fragments from an aphyric tephriphonolite from the Siebengebirge [*Przybyla*, 2013]. (e, f) 19.2 mg amphibole from a basanite from the Rhön volcanic province, Central Germany [from *Mayer et al*., 2014]. (g, h) 12.2 mg K-feldspar from a latite from the Siebengebirge, Central Germany [*Przybyla*, 2013]. (i, j) 192.1 mg *K*-poor (*K* = 0.02 wt%) amphibole from a plagiogranite from the Oman ophiolite. Measured signal intensities and ratios are given as supporting information. Ages were calculated using HDB1 [24.21 ± 0.31 Ma; *Hess and Lippolt*, 1994] and Fish Canyon tuff sanidine [28.305 ± 0.036 Ma; *Renne et al*., 2010] as fluence monitors and using the decay constants given in *Renne et al.* [2010].

© 2014. American Geophysical Union. All Rights Reserved.

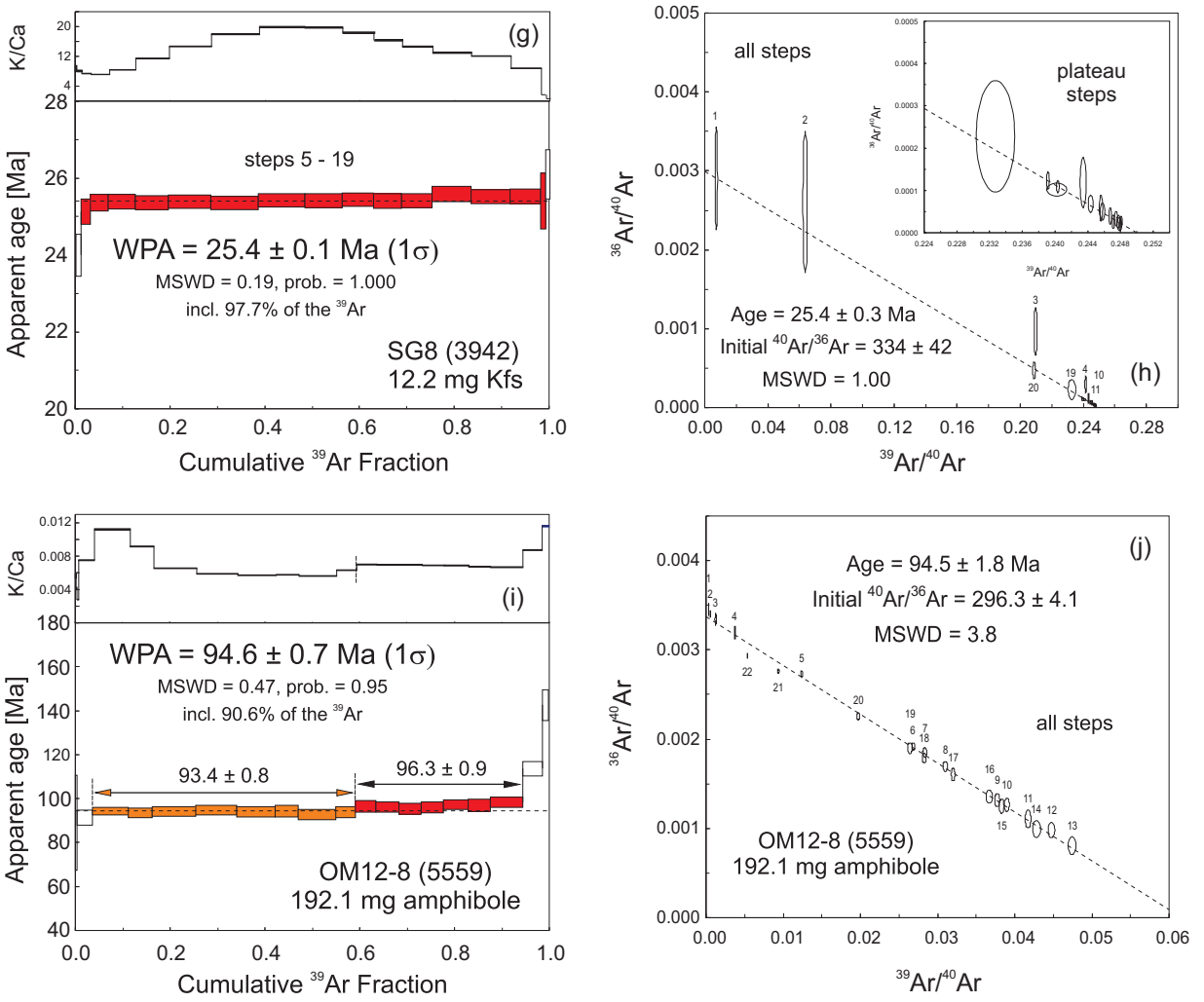

Figure 9. (Continued)

4. Conclusions

Our new sample-transfer system and low-volume high-temperature cell provide the potential to gain high-resolution age spectra from a variety of samples, allowing extraction of reliable $^{40}Ar/^{39}Ar$ ages in many cases. It does not redundantize careful sample preparation, which is the prerequisite of any approach of high-quality data acquisition. The disadvantage of the system—the release of small quantities of atmospheric Ar from the Mo-crucibles during step heating—is compensated by the correction for atmospheric Ar and has no measurable influence on the results. Due to the highly reproducible and homogeneous temperature distribution, the absence of chemical disequilibrium during sample degassing, the overall low blank level, and the very short baking time, the system is predominantly suitable for high-resolution $^{40}Ar/^{39}Ar$ dating of young and/or K-poor samples and for the determination of Ar diffusion parameters in minerals. These advantages—along with the low volume and the possibility to remove the degassed sample residue after measurement—make the system also suitable for all other applications in $^{40}Ar/^{39}Ar$ geo-thermochronology that require highly reproducible temperature conditions as well as large sample quantities.

Appendix A: Temperature Calibration

See Figure A1.

© 2014. American Geophysical Union. All Rights Reserved.

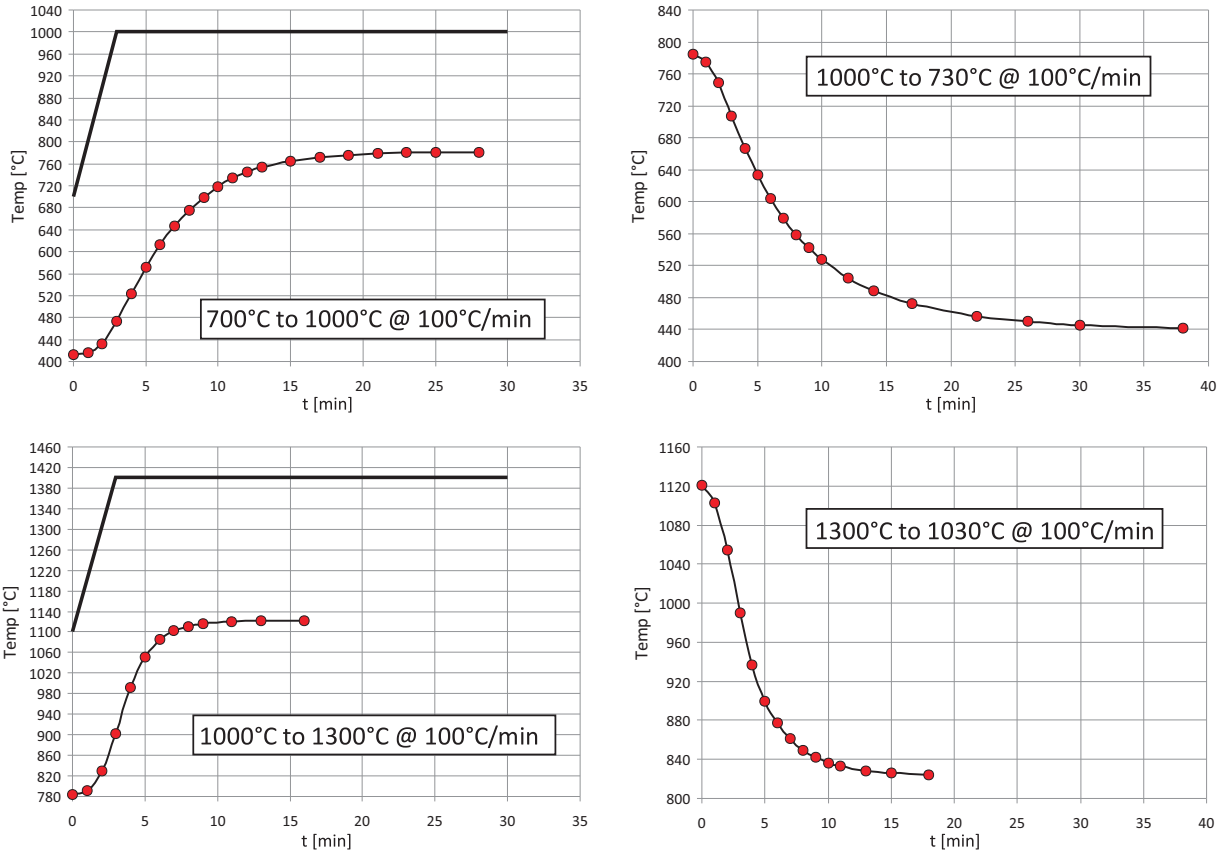

Figure A1. Temperature rise *inside* a sample crucible and time required to reach thermal equilibrium between heating element and inner part of an (empty) sample crucible. Exemplary shown are two heating curves, and two cooling curves. Note that at higher temperatures thermal equilibrium between inner and outer part of the HTC is achieved significantly faster (at an equal heating/cooling rate of 100°C/min). Black lines in the heating diagrams: Outer temperature.

Appendix B: Crucible Cleaning

To remove glass residues from the Mo-crucibles, we use concentrated HF and ultrasonicate the crucibles in a closed Savillex® beaker every 3 h for 15 min over a period of 3–6 days without changing the HF. The presence of oxidizing agents (e.g., nitric acid) in the HF should be avoided to prevent the formation of Mo-oxide. After this procedure, the glass residues are dissolved, typically leaving a white precipitate of insoluble fluorides, but the crucibles may have a light brownish to gray coating of Mo-oxide due to the presence of air oxygen in the HF. After rinsing the crucibles repeatedly in water, this Mo-oxide coating is removed by treating the crucibles for a few minutes with a cold mixture of concentrated ammonium acid (25–30%) and hydrogen peroxide (∼4:1 to 5:1) in an ultrasonic bath. After rinsing in deionized water and drying, the crucibles are baked at >1500°C in UHV for >30 min to remove atmospheric Ar. Due to the polycrystalline nature and structural defects in Mo, the crucibles will slowly take up atmospheric Ar after baking. Storage should thus be in UHV, or, ideally, crucibles should be loaded and used shortly after baking.

Appendix C: Moles From Signals

Moles Ar (n_i) in the preparation system and mass spectrometer for each temperature step are calculated from the measured signal intensities according to:

$$n_i = \frac{U \times V_A \times 133}{R_A \times S \times R \times T} \times \frac{V_A + V_p}{V_A},$$

where U is the signal intensity in Volt, V_A the volume of the ARGUS in m^3 (∼6.17×10^{-4} m^3), V_p the volume of the preparation system in m^3 (∼4.21×10^{-4} m^3 without HTC), R_A the universal gas constant (8.314472 J

© 2014. American Geophysical Union. All Rights Reserved.

mol^{-1} K^{-1}), S the sensitivity of the mass spectrometer in A/Torr (~1.1–1.3 × 10^{-3} A/Torr dependent on tuning), R the resistivity of the Faraday-amplifier system in Ω, and T the absolute temperature. The constant 133 transforms the sensitivity to SI units (A/Pa).

To calculate the total amount of Ar released per temperature step from a sample (or crucible), the volume of the HTC system (V_{HTC} ~2.52 × 10^{-4} m^3) needs to be considered as follows:

$$n_{tot} = n_i \times \frac{V_p + V_{HTC}}{V_p} \approx 1.6 \times n_i.$$

This is due to the fact that the valve between the HTC and the preparation system is closed after heating, i.e., prior to the expansion of the purified Ar into the mass spectrometer.

Appendix D: Gas Purification

The gas purification system (preparation system) is built around a steel block (central unit) that comprises the getters and connects the periphery (furnace, laserport, mass spectrometer) via CF16 flanges. It is pumped by a Pfeiffer TMU071 turbo pump, backed by an oil-free diaphragm pump, and a Varian Starcell Vaclon Plus 55 ion getter pump. The clear diameter of the drill holes inside the central unit and of the tubing to the periphery—including the mass spectrometer—is 8 mm. Gas purification is achieved by two SAES GP50 getter pumps equipped with St101 nonevaporable cartridges, assembled in water cooled housings and mounted to the central unit via two manual CF16 VAT valves. One of the getters operates at room temperature to reversibly adsorb hydrogen, one is at ~400°C to irreversibly adsorb active gases (N_2, O_2, H_2O, CO, CO_2) and to thermally crack and adsorb molecules such as hydrocarbons (see www.saesgetters.com). Generally, the pumping efficiency for hydrocarbons is significantly less than for other active gases. The volume of the preparation system—including the getters and the inlet valve to the mass spectrometer—is ~421 mL.

Appendix E: Hardware Integration and System Automation

The major hardware control unit is a software packet delivered by GV Instruments as part of the ARGUS (Figure 4). This packet comprises the *IonVantage*, the *Noble*, and the *PrepSequencer programs*. *Noble* allows to control and optimize the source parameters, and to directly control the 20 DC outputs (+24 V) of the ARGUS I/O interface, either manually or by the *PrepSequencer*. The *PrepSequencer*—along with the DC outputs of the ARGUS—is used for automated measurements (Figure 4). Each blank, airshot, or temperature step measurement makes a single line in the sample list of the *IonVantage* program and is associated with a set of files: (i) the tuning parameter file, defining the source settings; (ii) the method file, comprising the data acquisition details; and (iii) the inlet file, containing the whole preparation sequence (getter time, degassing time, etc.). The sample list is executed line by line. Each experiment (i.e., line) calls the *PrepSequencer*, which then executes the series of commands defined in the inlet file, i.e., opens, closes valves, and triggers the laser or HTC control units via the ARGUS I/O interface. Waiting segments in the inlet file allow variable degassing and getter time setting, and are used to wait for external processes (laser or HTC degassing steps, data acquisition) to be finished. After degassing, gas purification, and gas inlet, the *PrepSequencer* starts the data acquisition, followed by postacquisition pumping. Finally, the *PrepSequencer* returns the control to *IonVantage*, which then executes the next line in the sample list (i.e., the next heating step, blank, or airshot).

An in-house developed LabView software controls the HTC. The individual temperature steps triggered by the *PrepSequencer* are ramped from a defined base temperature with a distinct heating rate (usually 100°C/min); then they are hold for the given heating time. After dwell, the temperature is driven to a base temperature, which is dynamically adopted to be 300°C below the next heating step.

© 2014. American Geophysical Union. All Rights Reserved.

Acknowledgments

The data shown in the figures of this paper, as well as the Matlab software used for data reduction, are available from the first author upon request. The raw data used to calculate the $^{40}Ar/^{39}Ar$ age spectra and inverse isochron diagrams in Figure 9 (time zero intercept values for blank and temperature steps, decay constants, interfering isotope correction factors, etc.) are given as supporting information. The Deutsche Forschungsgemeinschaft (DFG) and the Sächsische Ministerium für Wissenschaft und Kunst (SMWK) funded the ALF facility via equipment and basic research grants. Maria Herrmann provided sample OM12-8 and related petrographic information. Operation and maintenance of the facility would not be possible without the technical support provided by Tino Beyer and Udo Böhme from the electrical workshop of the TU Bergakademie Freiberg. Andreas Schramm, Marion Seefeld, and Mario Lapke from the mechanical workshop remodeled with unremittingly patience any kind of mechanical component. Anja Obst assisted sample handling and preparation. Daniel Rutte critically but constructively commented the lab's workflow and measurement protocols. The reactor services team in Rez, Czech Republic, performed the neutron irradiations. Many thanks to Thomas Przybyla and Carsten Münker for providing the samples from the Siebengebirge. Constructive reviews by Fred Jourdan, Jan Wijbrans, and Huaiyu He helped to improve the manuscript and are greatly appreciated. Janne Blichert-Toft is thanked for editorial handling.

References

Cassata, W. S., and P. R. Renne (2013), Systematic variations of argon diffusion in feldspars and implications for thermochronometry, *Geochim. Cosmochim. Acta*, *112*, 251–287.

Coble, M. A., M. Grove, and A. T. Calvert (2011), Calibration of Nu-Instruments Noblesse multicollector mass spectrometers for argon isotopic measurements using a newly developed reference gas, *Chem. Geol.*, *290*(1–2), 75–87.

Dodson, M. H. (1973), Closure temperature in cooling geochronological and petrological systems, *Contrib. Mineral. Petrol.*, *40*, 259–274.

Duncan, R. A., P. R. Hooper, J. Rehacek, J. S. Marsh, and A. R. Duncan (1997), The timing and duration of the Karoo igneous event, southern Gondwana, *J. Geophys. Res.*, *102*, 18,127–18,138.

Hess, J. C., and H. J. Lippolt (1994), Compilation of K-Ar measurements on HD-B1 standard biotite. 1994 Status report, *Panerozoic Time Scale, Bull. Liais. Inform. IUGS Subcom. Geochron.*, *12*, 19–23.

Jourdan, F., G. Féraud, H. Bertrand, M. K. Watkeys, and P. R. Renne (2007), Distinct brief major events in the Karoo large igneous province clarified by new $^{40}Ar/^{39}Ar$ ages on the Lesotho basalts, *Lithos*, *98*, 195–209.

Jourdan, F., A. Marzoli, H. Bertrand, S. Cirilli, L. H. Tanner, D. J. Kontak, G. McHone, P. R. Renne, and G. Bellieni (2009), $^{40}Ar/^{39}Ar$ ages of CAMP in North America: Implications for the Triassic–Jurassic boundary and the ^{40}K decay constant bias, *Lithos*, *110*, 167–180.

Jourdan, F., W. D. Sharp, and P. R. Renne (2012), $^{40}Ar/^{39}Ar$ ages for deep (~3.3 km) samples from the Hawaii Scientific Drilling Project, Mauna Kea volcano, Hawaii, *Geochem. Geophys. Geosyst.*, *13*, Q05004, doi:10.1029/2011GC004017.

Koppers, A. A. P., R. A. Duncan, and B. Steinberger (2004), Implications of a nonlinear $^{40}Ar/^{39}Ar$ age progression along the Louisville seamount trail for models of fixed and moving hot spots, *Geochem. Geophys. Geosyst.*, *5*, Q06L02, doi:10.1029/2003GC000671.

Lovera, O. M., F. M. Richter, and T. M. Harrison (1989), The $^{40}Ar/^{39}Ar$ thermochronometry for slowly cooled samples having a distribution of diffusion domain sizes, *J. Geophys. Res.*, *94*(B12), 17,917–17,935.

Lovera, O. M., F. M. Richter, and T. M. Harrison (1991), Diffusion domains determined by ^{39}Ar released during step heating, *J. Geophys. Res.*, *96*(B2), 2057–2069.

Ludwig, K. R. (2012), *User's manual for Isoplot 3.75: A Geochronological Toolkit for Microsoft Excel*, 75 pp. Berkeley Geochronology Center, Special Publication No. 5, Berkeley.

Mark, D. F., D. Barfod, F. M. Stuart, and J. Imlach (2009), The ARGUS multicollector noble gas mass spectrometer: Performance for $^{40}Ar/^{39}Ar$ geochronology, *Geochem. Geophys. Geosyst.*, *10*, Q0AA02, doi:10.1029/2009GC002643.

Mayer, B., Jung, S., Romer, R.L., Pfänder, J.P., Klügel, A., Pack, A., and Gröner, E. (2014), Amphibole in alkaline basalts from intra-plate settings: Implications for the petrogenesis of alkaline lavas from the metasomatised lithospheric mantle, *Contrib. Mineral. Petrol.*, *167*(3), 1–22.

McDougall, I., and T. M. Harrison (1999), *Geochronology and Thermochronology by the $^{40}Ar/^{39}Ar$ Method*, 269 pp., Oxford Univ. Press, Oxford.

Przybyla, T. (2013), $^{40}Ar/^{39}Ar$-Datierungen an Vulkaniten des Siebengebirges, M.Sc. thesis, Universität zu Köln, Germany.

Renne, P. R., R. Mundil, G. Balco, K. Min, and K. R. Ludwig (2010), Joint determination of ^{40}K decay constants and $^{40}Ar^*/^{40}K$ for the Fish Canyon sanidine standard, and improved accuracy for $^{40}Ar/^{39}Ar$ geochronology, *Geochim. Cosmochim. Acta*, *74*(18), 5349–5367.

© 2014. American Geophysical Union. All Rights Reserved.